Qualitative and quantitative determination of gas species in samples representing atmospheres by infrared spectroscopy

by Martin Mueller – The Open University, April 18, 2023

Introduction

Knowledge of the composition of atmospheres of celestial bodies is of great interest, with respect to Earth to understand and predict the climate and to study biochemical cycles, with respect to other planets and moons to search for life. Today many techniques are available, among others mass spectroscopy, Raman spectroscopy, ultraviolet–visible spectroscopy and infrared spectroscopy. All of them have strengths and weaknesses and certain areas of application. In this experiment, infrared spectroscopy was used, which exploits the property of molecules with electric dipole moment to absorb electromagnetic radiation in their resonant frequencies. The energy absorptions depend on the structures of the molecules and their different vibrational modes, but they are all quantized so that the characteristic absorption peaks can be used to determine the types of molecules. Using Dalton's law, Beer-Lambert's law, and the ideal gas law in combination with known absorption spectra of reference gases, the abundances can be calculated (The Open University, 2022a).

A limitation of infrared spectroscopy is that it can only be used to determine infrared active molecules, i.e. it is not suitable for monatomic gases such as helium or argon and infrared inactive molecules such as O_2, N_2, H_2. The advantages of infrared spectroscopy are that it is non-invasive and can be performed without physical samples using infrared telescopes.

The question to be answered is: Within the limits of infrared spectroscopy and specific experimental constraints, can the types and abundances of gas species in two unknown samples A and B, produced by the Open University to simulate atmospheres, be determined with sufficient precision to allow inferences about hypothetical planets or moons of origin?

Methods and results

Theory

As depicted in Figure 1, the theories and laws applied in this experiment concern the measurements (1) and the data analysis and calculations (2).

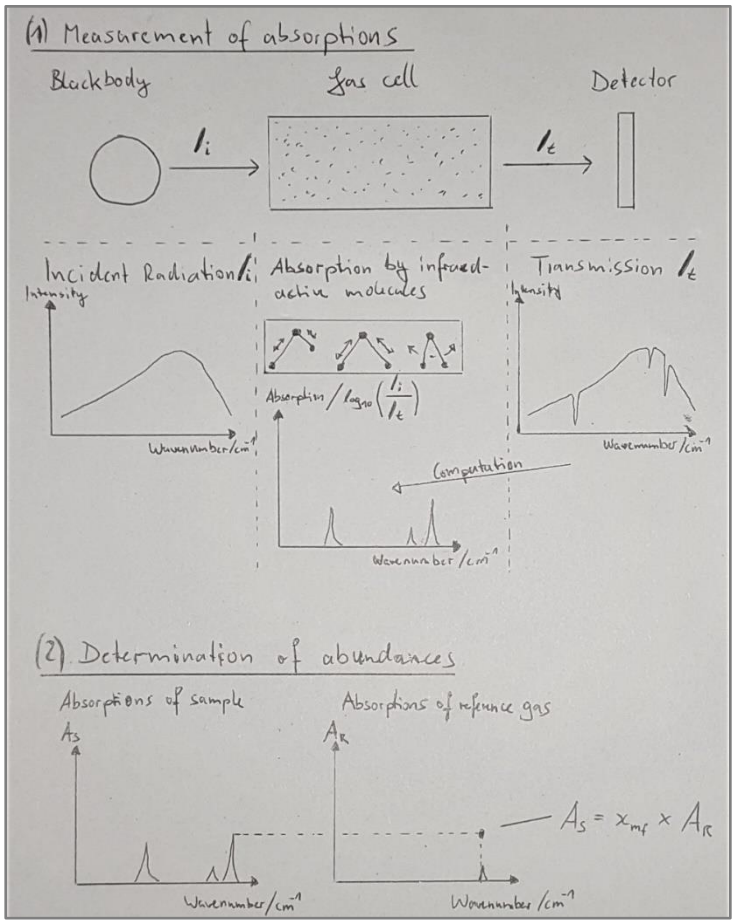

Figure 1: Schematic representation of the laws used to measure absorptions (1) and determine abundances (2). A blackbody is used to pass infrared radiation I_i through a gas cell in which molecules absorb some of the radiation due to different vibrational modes (only three are shown here, namely asymmetric and symmetric stretching and bending). Gaps in the transmissions I_t are detected and processed as absorption values A_s. Abundances and finally partial pressures are calculated by determining mapping factors x_{mf} applied to temperature adapted absorption values A_R of a reference gas.

The measurement phase of the experiment builds on the theory that molecules absorb quantized energies from electromagnetic radiation with resonance frequencies corresponding to molecular vibrational degrees of freedom. Absorptions of vibrational energy quanta only take place in the infrared spectrum of the electromagnetic spectrum. They also require electric dipole moments in the molecules, so that absorptions do not occur in monatomic gases and gases consisting of molecules with equal charge distributions. In practice, when infrared radiation passes through a gas cell, the allowed absorptions can be detected as the reciprocal of the transmission gaps.

In the analysis phase of the experiment, where the determination of the abundances is needed, combinations of laws are involved. According to Dalton's law, the total pressure of a gas mixture ***P*** is the sum of the partial pressures $\boldsymbol{p_g}$ of its individual gases ***g***, that is

$$P = p_1 + p_2 + p_3 + \cdots + p_n \qquad (1)\,.$$

According to the Beer-Lambert law and by applying Dalton's law and the ideal gas equation, the logarithmic transmission-to-absorption ratio $\boldsymbol{A_g}$ of a mixed gas constituent is proportional to its partial pressure $\boldsymbol{p_g}$, that is

$$A_g = \frac{\epsilon l}{RT_g} \times p_g \qquad (2)\,,$$

where $\boldsymbol{\epsilon}$ is the molar absorption coefficient, ***l*** is the length of the gas cell, ***R*** is the molar gas constant, $\boldsymbol{T_g}$ is the gas temperature and

$$A = \log_{10}\frac{I_i}{I_t} \qquad (3)\,,$$

where $\boldsymbol{I_i}$ is the incident radiation and $\boldsymbol{I_t}$ is the transmitted radiation.

In conjunction with reference gases of known absorptions at defined pressures and same temperatures, partial pressures can be calculated for individual gases in gas mixtures by visually determining or computing a mapping factor x_{mf} due to the relationship

$$A_g = x_{mf} \times A_R \qquad (4)\,,$$

where A_R is the absorbance of a reference gas at the same temperature at which A_g was measured.

These laws finally allow to calculate relative abundances $Abundance_{rel}$ of the species in gas samples:

$$Abundance_{rel_g} = \frac{p_g}{P} \qquad (5)\,.$$

Experimental equipment

As depicted in Figure 2 the experimental setup included two main physical units controlled by several computer programs (The Open University, 2022b):

- The gas storage and control system allowed the gas cell to be filled with the test gas CO_2 or the desired gas mixture at precise pressures. Key instrument to physically control the pressures was the thermal valve, an instrument developed by The Open University and used for the Rosetta mission.
- The IR source and interferometer generated the controlled radiation that was passed through a gas cell, then detected by a detector and converted by a Fourier transform algorithm.

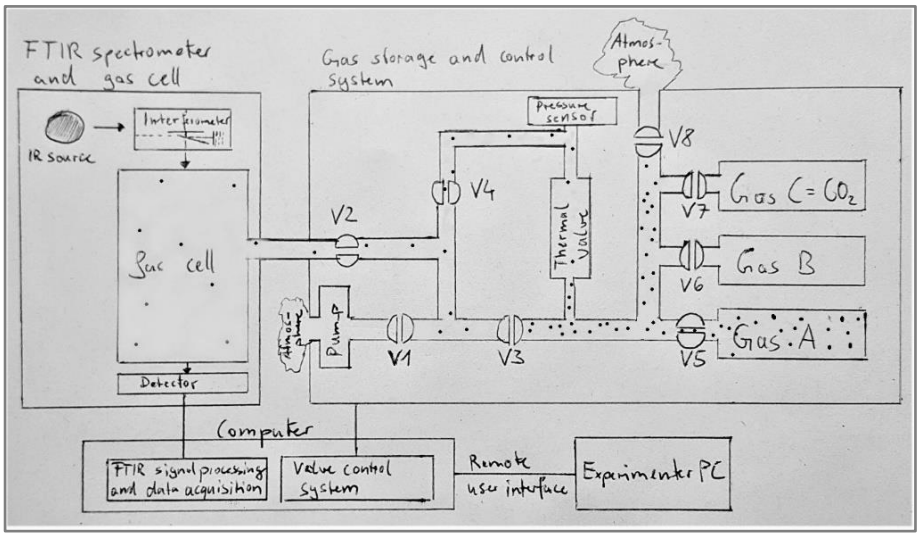

Figure 2: Diagram showing the experimental setup. V1 to V8 are controllable valves in addition to the central element, the thermal valve. Here the situation is shown in which the gas from sample A filled the gas cell with the pressure as defined via the thermal valve. The amount of gas is represented by small dots.

Experiment and data analysis

The experiment was conducted under the guidance of the Open University study material. Two separate sessions were executed, each containing essential activities for the entire experiment and each limited to a duration of 90 minutes. The first session included the calibration of the pressure sensor, the characterization of the thermal valve and the measurement of a CO_2 absorption spectrum at various pressures (The Open University, 2022c). The results from the first session were used to plan the second session. In the second session spectra of the unknown gas samples A and B at different pressures were measured (The Open University, 2022d). The experiment could be divided into five successive steps.

Step 1: Planning session 1 and executing it by calibrating the pressure sensor, actuating the thermal valve and measuring the absorption spectra of the test gas CO_2

Session 1 was planned in detail by a team of two students consisting of Mark Rapson and the author of this report, Martin Mueller, and by considering time and technical constraints.

An essential part of the gas storage and control system was a pressure sensor, which was needed for the precise control of the thermal valve. The system was handed over in an uncalibrated state and due to the limited time, it was decided to perform a 2-point calibration, by

- reading the current atmospheric pressure in Milton Keynes, where the equipment was located and converting it into mbar,
- evacuating the gas line that was directly connected to the pressure sensor,
- reading the pressure sensor ADC value (a 16-bit number of an analogue to digital converter) corresponding to 0 mbar,
- filling the system with air to reach atmospheric pressure,
- reading the pressure sensor ADC value corresponding to the atmospheric pressure, and
- calculating the calibration values. The gas storage and control system required m and c values for the calibration, representing a linear relationship of the form ***mbar = m x ADC + c*** between both ADC and both mbar values. This was calculated by a prepared Python program with the advantage to potentially include more values and to quickly include error values. An analogous manual calculation for m and c with the values noted in the experiment is:

$$m = \frac{\Delta\, mbar}{\Delta\, ADC} = \frac{1009 - 0}{5792 - 545} = 0.1923\ (4\ s.f.) \qquad (6)$$

$$c = 0 - 545 \times m = -104.8\ (4\ s.f.) \qquad (7)\ .$$

  Since the estimated errors for the mbar and ADC values, 0.1 and 1.0, respectively, were small, Python provided the same values to 4 s.f. as in the manual calculation.

A necessity for obtaining reproducible results and later calculating the abundances of the individual gases was the capability to set accurate pressures in the gas cell. The sensitive instrument for this was the thermal valve. Before deploying it in the main experiment, a characterization was performed to determine the exact actuation temperature of the valve. This characterization was automatically stored by the system and applied for all subsequent activities.

In a final activity in Session 1, the absorption spectra for the test gas CO_2 were measured at various pressures. The pressures chosen by the team were 10 mbar, 30 mbar, 40 mbar, 50 mbar, 60 mbar, 70 mbar, 100 mbar, 110 mbar, 120 mbar, 130 mbar, 140 mbar, and 150 mbar. The pressures were carefully selected so that as many and as varied pressures as possible could be processed in the limited experimental time.

Step 2: Determining the absorption limit up to which the detector works properly

One result of Session 1 were 13 absorption spectra of pure CO_2 gas at different pressures. In a subsequent analysis, the absorption peaks of the asymmetric stretching of CO_2 molecules at wavenumber 2349 were determined at each pressure and plotted appropriately. According to the Beer-Lambert law, there is a linear relationship between absorption values and pressures. As can be seen in Figure 3, this linear relationship exists only up to absorbance values of about 0.6 -0.7, after which the absorbance increases non-linearly. This is due to the limited sensitivity of the detector at low transmittances. One consequence of this analysis was to plan pressures for the second session that would not cause the absorbance values to exceed 0.7.

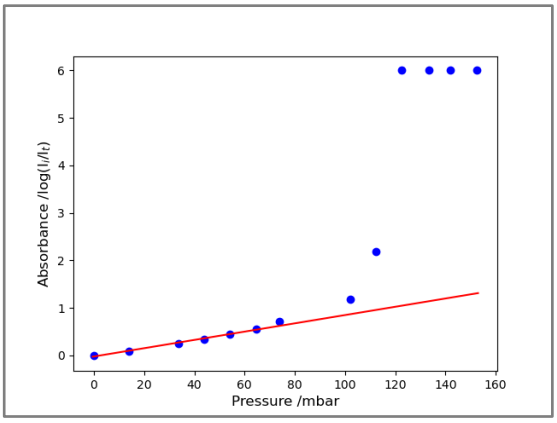

Figure 3: Visual representation of the determination of the absorption limit to which the detector operates properly. The analysis showed that a straight line fit would have the lowest R^2 values for absorbance values from 0 to 0.6-0.7. Here, the best-fit line (red) was calculated through the first 6 data points from 0 mbar to 64.7 mbar.

Step 3: Planning session 2 and executing it by scanning spectra for gas samples A and B, each at carefully selected pressures

The plan developed by the team for session 2 was to start with a low-pressure scan at 10 mbar, read the absorbance value for the peak of interest, calculate a factor to reach the target absorbance value of 0.6-0.7, and multiply the initial pressure by it. Then 3-4 scans should be performed at similar pressures in 10% increments to stay within this optimal pressure range and collect them for later statistical processing. In the experiment, however, it turned out that the scans took an unexpectedly long time, about 10 minutes each, much longer than in session 1. Therefore, only 4 scans could be performed for each sample, and it was decided during the experiment to perform them at pressure ranges spread as far as possible. Since the team ran out of time, the last scan for sample B was performed at 800 mbar instead of the maximum possible value of 1000 mbar, which would have been more favorable. Data from all scans, including background scans at 0 mbar have been downloaded for the subsequent analysis. The raw data plots are shown in Figures 4 and 5.

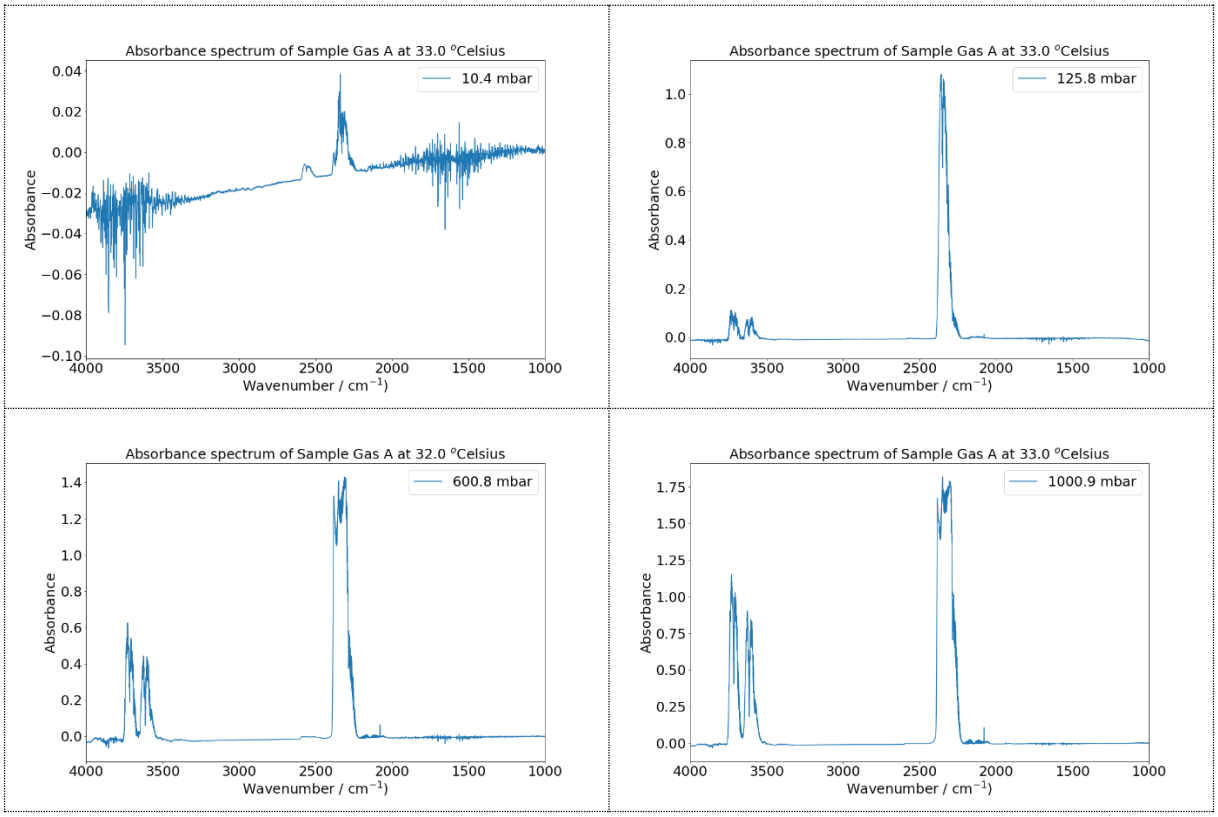

Figure 4: All scans of gas sample A, which served as input for the later in-depth analysis. At first glance, it can be seen that the scan at 10 mbar has a strong noise-to-absorption ratio and that the absorption peaks at pressures of 600 and 1000 mbar are strongly saturated at a wavenumber around 2400. The spectra at higher pressures are dominated by CO_2 peaks between wavenumbers 4000 and 3500 and 2500 and 2000. CO can be seen as very small elevations to the right of the highest CO_2 peak.

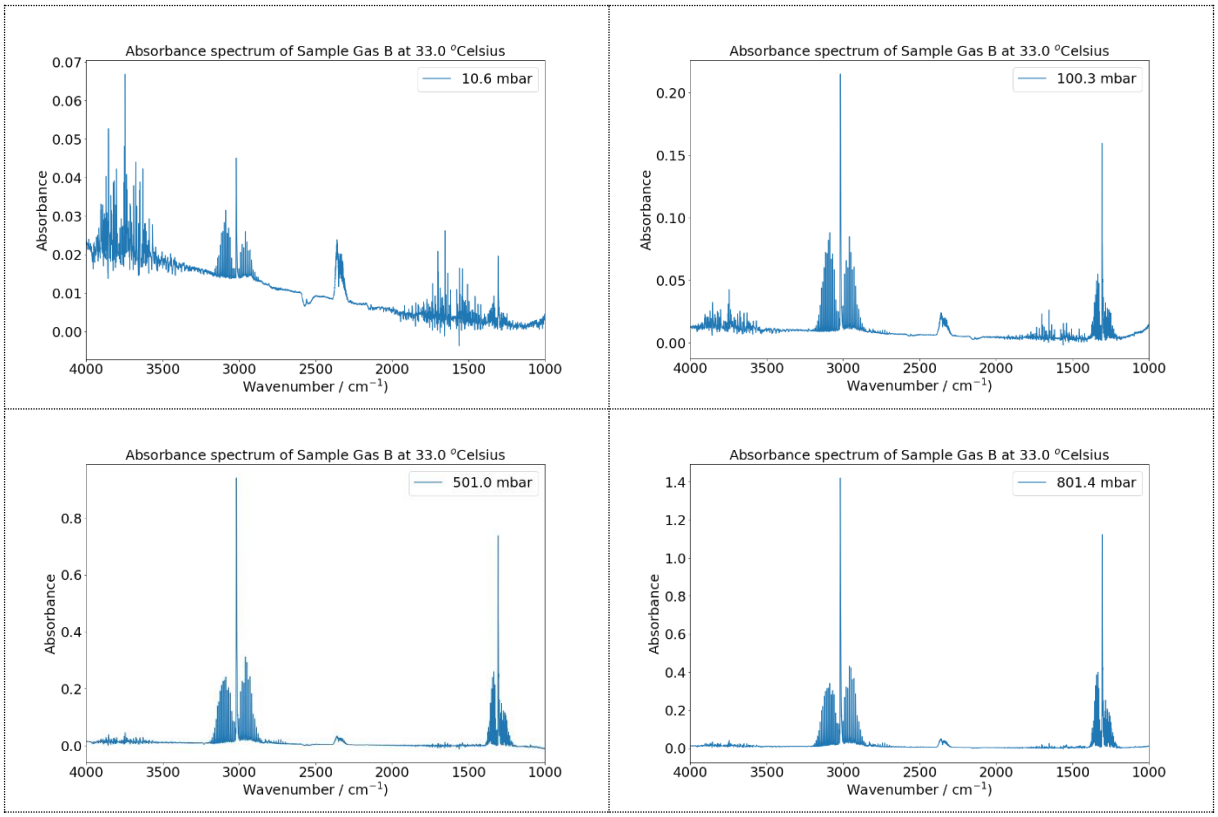

Figure 5: All scans of gas sample B, which served as input for the later in-depth analysis. At first glance, it can be seen that the scan at 10 mbar has a strong noise to absorption ratio. The spectra at higher pressures are dominated by CH_4 peaks at wavenumber 3000 and between wavenumbers 1500 and 1000. CO_2 can be seen as a very small elevation at a wavenumber of about 2400.

Step 4: Identifying potential gas species in samples A and B (qualitative analysis)

After scanning, the data was plotted using Python, and the areas of the peaks were magnified and compared to the absorption spectra of reference gases likely to be found on planets and moons. The Open University provided some Python programs for this purpose, which were adapted to the own needs. Likewise, it supplied spectra of the reference gases, C_2H_6, CH_3OH, CH_4, CO, CO_2, H_2O, NH_3 (The Open University, 2022e). The results of the qualitative analysis can be found in columns 2 - 7 of tables 1 and 2 respectively.

Initially, H_2O was suspected in both samples, but the peaks did not show a linear relationship with higher pressures, suggesting that the H_2O remained after evacuation of the gas cell. Therefore, H_2O was excluded from further consideration.

In sample A, a peak at wavenumber 2077 was identified that was linearly related to pressure. It matched a peak of the reference gas CO_2, but it could not be identified as a vibrational mode (National Institute of Standards and Technology, 2023). It could have originated from a foreign gas that was contained in the CO_2 cylinder used for mixing the samples.

1	2	3	4	5	6	7	8	9	10	11
	Qualitative analysis						Quantitative analysis			
Pressure of scan /mbar	Start WN /cm^{-1}	End WN /cm^{-1}	Peak WN /cm^{-1}	Initial guess of potential gas	Peak absorbance (baseline corrected)	Vibrational modes of molecules	Ref. pres-sure /mbar	Factor ref. gas	Partial pressure of sample /mbar	Portion in sample
10.4	2394	2230	2336	CO_2	0.049	CO2_2	51.8	0.11	5.7	54.8%
125.8	3752	3670	3730	CO_2	0.12	CO2_1_1	51.8	2.3	119.1	94.7%
	3647	3543	3595	CO_2	0.087	CO2_1_2	51.8	2.35	121.7	96.8%
	2394	2230	2356	CO_2	1.09	CO2_2	51.8	2.65	137.3	109.1%
	2191	2081	2116	CO	0.006	CO	289.5	0.007	2.0	1.6%
	2079	2074	2077	CO_2	0.013	CO2_3	51.8	2.4	124.3	98.8%
600.8	3760	3647	3729	CO_2	0.63	CO2_1_1	51.8	11	569.8	94.8%
	3655	3455	3624	CO_2	0.44	CO2_1_2	51.8	10.9	564.6	94.0%
	2400	2220	2305	CO_2	1.43	CO2_2	Detector saturated, no mapping possible			
	2214	2080	2169	CO	0.024	CO	289.5	0.030	8.7	1.4%
	2080	2075	2077	CO_2	0.073	CO2_3	51.8	11.1	575.0	95.7%
1000.9	3759	3670	3729	CO_2	1.16	CO2_1	51.8	21.8	1129.2	112.8%
	2397	2222	2348	CO_2	1.82	CO2_2	Detector saturated, no mapping possible			
	2213	2080	2169	CO	0.03	CO	289.5	0.055	15.9	1.6%
	2080	2075	2077	CO_2	0.11	CO2_3	51.8	17.7	916.9	91.6%

Table 1: Overview of the scans performed for gas sample A (column 1) and outcome of the applied qualitative and quantitative analysis (columns 2-7 and columns 8-11 respectively). Initial guesses about possible gases (H_2O) that turned out to be noise or unquantifiable were removed from this table to present only data relevant to closer examination. Absorption peaks below a threshold (<0.05) and above a threshold (> 1.0) are greyed out. Even though all peaks for CO are below an absorption of 0.05, the data is kept since no other is available (see interpretation section of this report). Columns 2 and 3 indicate the range of wavenumbers (WN) in which a peak (column 3) could be detected. Column 7 shows the association of the vibrational modes with the peaks as identified from high wavenumbers to low wavenumbers. CO2_1_1 and CO2_1_2 are the two peaks of the CO_2 combination mode. CO2_2 is the asymmetric stretching mode of CO_2. CO2_3 is a peak that has a linear relationship with pressure, but which is not a CO_2 vibrational mode and therefore greyed out.

1	2	3	4	5	6	7	8	9	10	11
	Qualitative analysis						Quantitative analysis			
Pressure of scan /mbar	Start WN /cm^{-1}	End WN /cm^{-1}	Peak WN /cm^{-1}	Initial guess of potential gas	Peak absorbance (baseline corrected)	Vibrational modes of molecules	Ref. pres-sure /mbar	Factor ref. gas	Partial pressure of sample /mbar	Portion in sample
10.6	3172	2851	3017	CH_4	0.031	CH4_1	52.2	0.055	2.9	27.1%
	2400	2281	2359	CO_2	0.016	CO2_2	51.8	0.033	1.7	16.1%
	1400	1180	1307	CH_4	0.016	CH4_2	52.2	0.035	1.8	17.2%
100.3	3172	2851	3017	CH_4	0.21	CH4_1	52.2	0.35	18.3	18.2%
	2400	2281	2359	CO_2	0.018	CO2_2	51.8	0.040	2.1	2.1%
	1400	1180	1307	CH_4	0.16	CH4_2	52.2	0.030	1.6	14.8%
501.0	3172	2851	3017	CH_4	0.93	CH4_1	52.2	1.45	75.7	15.1%
	2400	2281	2359	CO_2	0.03	CO2_2	51.8	0.065	3.4	0.7%
	1400	1180	1307	CH_4	0.74	CH4_2	52.2	1.5	78.3	15.6%
801.4	3172	2851	3017	CH_4	1.4	CH4_1	52.2	2.1	109.6	13.7%
	2400	2281	2359	CO_2	0.045	CO2_2	51.8	0.105	5.4	0.7%
	1400	1180	1307	CH_4	1.1	CH4_2	52.2	2.4	125.3	15.6%

Table 2: Overview of the scans performed for gas sample B (column 1) and outcome of the applied qualitative and quantitative analysis (columns 2-7 and columns 8-11 respectively). Initial guesses about possible gases (H_2O) that turned out to be noise or unquantifiable were removed from this table to present only data relevant to closer examination. Absorption peaks below a threshold (<0.05) and above a threshold (> 1.0) are greyed out. Even though all peaks for CO_2 are below an absorption of 0.05, the data is kept since no other is available (see interpretation section of this report). Columns 2 and 3 indicate the range of wavenumbers (WN) in which a peak (column 3) could be detected. Column 7 shows the association of the vibrational modes with the peaks as identified from high wavenumbers to low wavenumbers. The concentration of CO_2 in sample B was too low to obtain reasonable absorbance values for its combination mode, which is why rows with CO2_1 have been eliminated. CH4_1 represents the degenerated stretching mode of methane and CH4_2 the degenerated bending mode.

Step 5: Determining the abundances of the identified gas species in samples A and B (quantitative analysis)

In the quantitative analysis the abundances of the identified gas species were determined. Two methods have been applied.

1.) Manually scaling reference gases of known pressure to the peaks in the samples to get mapping factors, calculate partial pressures and relate them to the pressures of the samples.

The manual scaling was done using a Python program. Examples are given in Figures 6 and 7. The results are listed in columns 9 of tables 1 and 2 respectively.

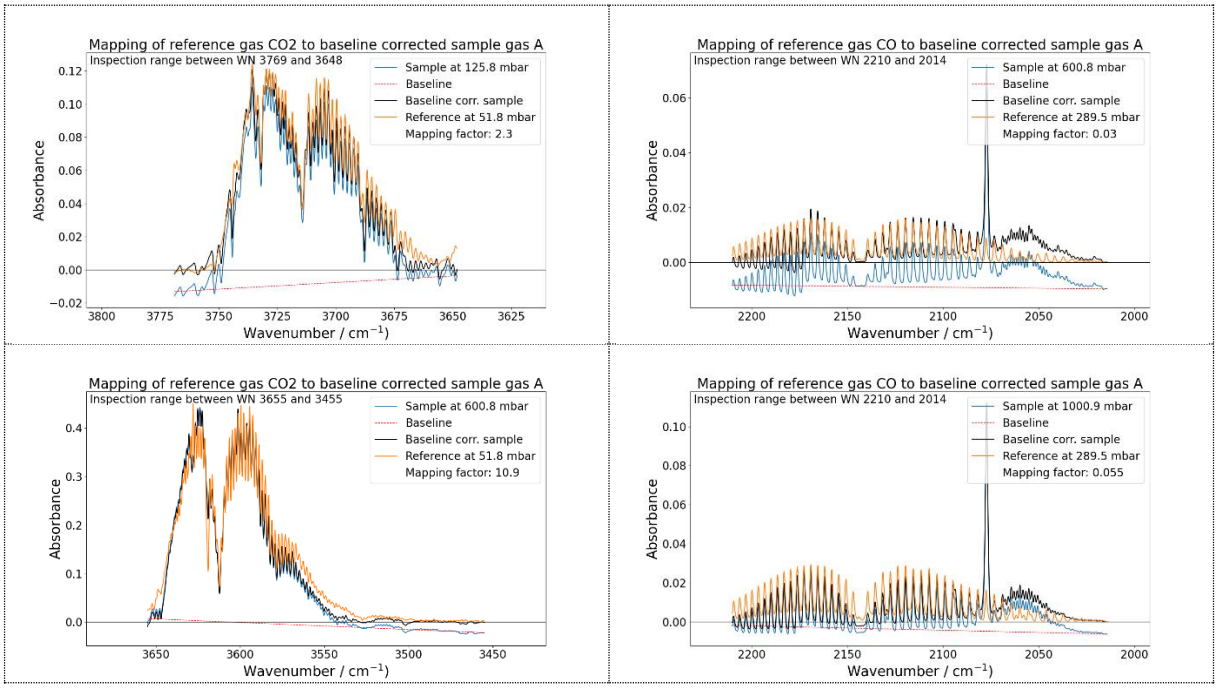

Figure 6: Scaled mapping of the temperature-corrected reference absorbances of CO_2 (left) and CO (right) onto the absorption spectrum of sample A. The regions of the peaks to be examined were cut out of the total spectrum for better investigation.

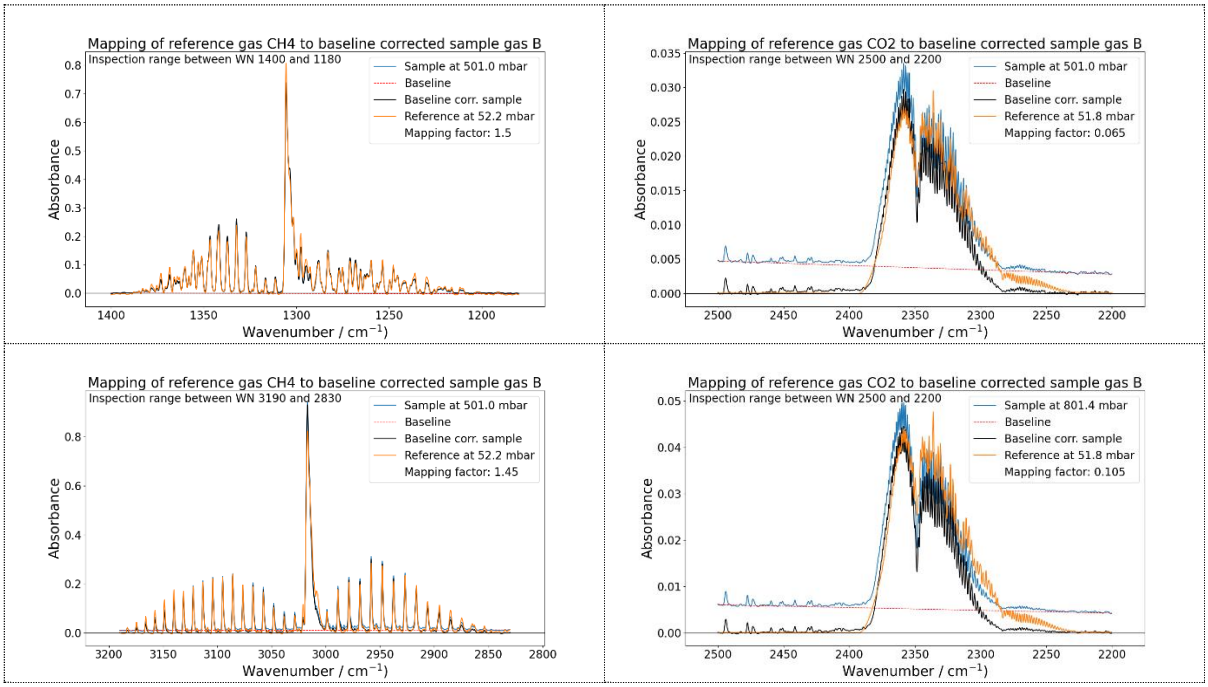

Figure 7: Scaled mapping of the temperature-corrected reference absorbances of CH_4 (left) and CO_2 (right) onto the absorption spectrum of sample B. The regions of the peaks to be examined were cut out of the total spectrum for better investigation.

After correcting the absorbances of the reference gases due to the temperature differences between the gas samples (33 °C) and the reference gases (22 °C),

$$A_{R_{33C}} = A_{R_{22C}} \times \frac{295.15\ K}{306.15\ K} \qquad (7)\ ,$$

from Equations 2 and 4 follows, that

$$p_g = x_{mf} \times\ p_R \qquad (8)\ ,$$

where x_{mf} is listed in columns 9 of tables 1 and 2 and p_g in columns 10.

Finally, the proportions are calculated according to Equation 5 and are listed in columns 11 of tables 1 and 2.

Averaging the proportions per species from the identified portions within the range of confidence (non-grayed out rows in tables 1 and 2) gave the final results of the abundances.

Sample A: 95.1% CO_2, 1.5% CO, 3.4% Undetermined

Sample B: 15.9% CH_4, 1.1% CO_2, 83% Undetermined

2.) Calculate the absorbances per peak of the individual peaks in the samples by least square linear regression over all pressures and relate them to the absorbances of the peaks in the reference gases

Analogous to step 2, the absolute peak values of absorbances of the sample scans were put into a linear relationship to filter out peaks outside of linearity and receive the relation

$$\frac{A_g}{mbar} \qquad (9)\ ,$$

as a result of the linear regression done by the Python program (equivalent to *m* of the straight line fit, since *c* = 0). Errors of 0.04 per peak due to according observed maximum noise in the background scans were included in the regression.

This relation was then put into relation to

$$\frac{A_R}{mbar} \qquad (10)\ ,$$

which finally provided the portions of the gas species per sample.

Peak	A_g/mbar (= *m*)	A_R/mbar	Portion
CO2-1-1	1.0555 x 10^{-3}	(0.0556 x 0.964)/51.8	102.0%
CO2-1-2	7.1747 x 10^{-4}	(0.0427 x 0.964)/51.8	90.3%
CO2-2	8.3053 x 10^{-4}	(0.0472 x 0.964)/51.8	94.5%
Average CO_2			**95.6%**

Peak	A_g/mbar (= m)	A_R/mbar	Portion
CH4-1	1.8392 x 10^{-3}	(0.5883*0.964)/52.2	16.9%
CH4-2	1.473 x 10^{-3}	(0.5576*0.964)/52.2	14.3%
Average CH_4			**15.6%**

Peak	A_g/mbar (= m)	A_R/mbar	Portion
CO	3.28 x 10^{-5}	(0.55 x 0.964)/289.5	**1.8%**

Peak	A_g/mbar (= m)	A_R/mbar	Portion
CO_2	4.4169 x 10^{-5}	(0.4722*0.964)/51.8	**0.5%**

Table 3: Abundances of species as calculated by the second method for sample A on the left and sample B on the right

The results from method 1 and 2 were averaged and are displayed in Figure 8.

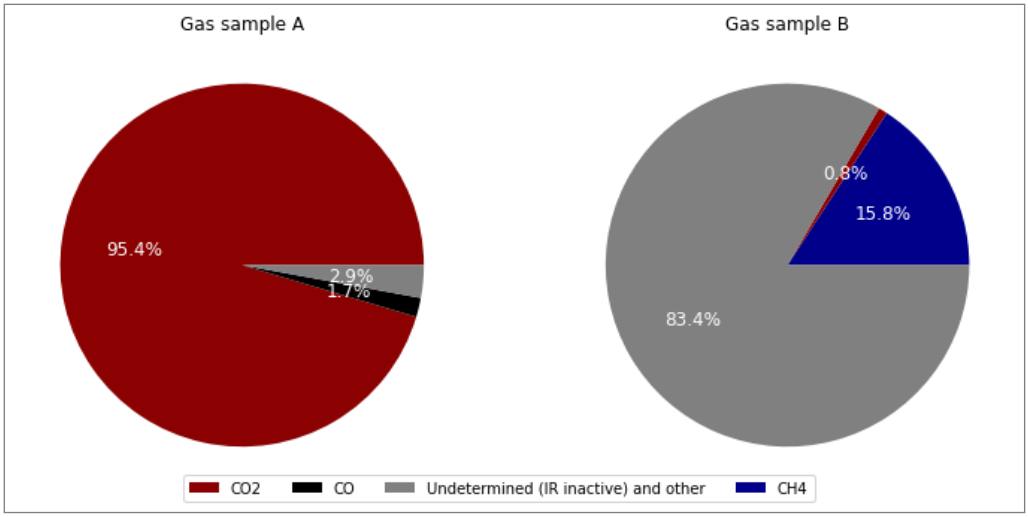

Figure 8: Averaged values from methods 1 and 2 for abundances of gas species in samples A and B

Discussion and interpretation

Both methods, as described in step 5, have advantages and disadvantages. While method 1 relies on subjective manual matching skills, method 2 is more statistical. Method 1 might be a better choice when only a few data are available, as was the case in this experiment. Method 2 could be an alternative or a supplement if many scans can be performed and it can be ensured that the absorptions of different gases do not overlap. Both methods gave similar results for the very abundant gases CO_2 and CH_4, which varied by only 0.5% and 1.9%, respectively. Much higher variations occurred for the trace gases CO and CO_2, ranging from 20% to 120%. From this and the fact that the low abundance gases consistently had very low absorbance values that were on the order of the background scan values (0.4 at the maximum), it can be assumed that the high abundance values are robust results, while the low abundance values are rather uncertain.

Noise was detected in both samples, possibly from water, perhaps just caused by condensed water in the gas cell, but in any case, not significant enough to be included in the results.

If one assumes that gas samples A and B represent atmospheres of known planets or moons, the analysis of gas sample A would be nearest to the atmospheres of Venus and Mars. The determined CO_2 abundances of 95.1% and 95.6% are closer to that of Mars (95.3%) than to that of Venus (96.5%). The determined CO abundances of about 1.5% and 1.8% are far from the tiny amounts on either planet (Mars: 0.07%, Venus: 0.002%). Given the uncertainties in the measurements and the fact that no traces of SO_2 were detected, which is present only on Venus, it is more likely that Sample A originates from Mars than from Venus.

Gas sample B undoubtably contains significant amounts of methane. This high amount is not found on any of known planets and moons with moon Titan having the most (3.5%). One explanation could be that the sample was taken as a snapshot at a location where methane was released due to geological activity and does not represent the average atmosphere. Another explanation could be that the sample comes from a yet unknown celestial body. This would be a sensational finding, since such a high amount of methane can be considered a biosignature of an exoplanet and a sign of life (Thomson, 2022).

Overall, however, it must be noted that the above interpretations are highly speculative, as only very few scans could be performed. Furthermore, since the samples were exposed only to infrared radiation, only infrared-active gas species could be detected. Spectroscopy at different wavelengths would be required to determine the other species.

Conclusions

- The question to be answered was whether the types and abundances of gas species in two unknown samples A and B could be determined by infrared spectroscopy with sufficient precision to allow conclusions to be drawn about hypothetical planets or moons of origin.

- In the experiment, only four, and thus many less scans than expected, could be performed per sample due to technical and time constraints.

- The analysis provided robust results for the high abundance of CO_2 in sample A, namely about 95-96%, and robust results for the abundance of CH_4 in sample B, namely about 16%, while the amounts of the low abundance gases, namely CO in sample A and CO_2 in sample B, are subject to large uncertainties.

- Gas sample A could have come from Mars or Venus, but it is more likely that it came from Mars.

- Gas sample B could not be assigned to any known planet.

- All interpretations are highly speculative since only a few scans could be performed. Especially for trace gases, more scans and at much higher pressures would give far better results with a lot less uncertainties.

References and acknowledgements

The Open University (2022a) 'Planetary science: Mars atmosphere'. *SXPS288-22J: Remote experiments in physics and space.* Available at: https://learn2.open.ac.uk/mod/oucontent/view.php?id=1926164 (Accessed 7 April 2023).

The Open University (2022b) 'Gas Cell operators manual'. *SXPS288-22J: Remote experiments in physics and space.* Available at: https://learn2.open.ac.uk/mod/oucontent/view.php?id=1926168 (Accessed 8 April 2023).

The Open University (2022c) '3.7 Calibrating the gas storage and delivery system based on the OU thermal valve'. *SXPS288-22J: Remote experiments in physics and space.* Available at: https://learn2.open.ac.uk/mod/oucontent/view.php?id=1926164&section=3.7 (Accessed 10 April 2023).

The Open University (2022d) '5.12 Carrying out the experiment'. *SXPS288-22J: Remote experiments in physics and space.* Available at: https://learn2.open.ac.uk/mod/oucontent/view.php?id=1926164&section=5.12 (Accessed 13 April 2023).

The Open University (2022e) 'Notebooks and sample files for Mars week 5'. *SXPS288-22J: Remote experiments in physics and space.* Available at: https://learn2.open.ac.uk/mod/folder/view.php?id=1926124 (Accessed 14 April 2023).

National Institute of Standards and Technology (2023) 'NIST Chemistry WebBook, SRD 69'. Available at: https://webbook.nist.gov/chemistry/ (Accessed 14 April 2023).

Thomson, M. et al. (2022) 'The case and context for atmospheric methane as an exoplanet biosignature', *Proceedings of the National Academy of Sciences*, 119 (14), Available at: https://doi.org/10.1073/pnas.2117933119 (Accessed 14 April 2023).